Journal of Solid Mechanics Vol. 6, No. 3 (2014) pp. 310-321

Implementing the New First and Second Differentiation of a General Yield Surface in Explicit and Implicit Rate-Independent Plasticity

F. Moayyedian, M. Kadkhodayan*

Mechanical Engineering Department, Ferdowsi University of Mashhad, Iran

Received 18 April 2014; accepted 20 June 2014

ABSTRACT

In the current research with novel first and second differentiations of a yield function, Euler forward along with Euler backward with its consistent elastic-plastic modulus are newly implemented in finite element program in rate-independent plasticity. An elastic-plastic internally pressurized thick walled cylinder is analyzed with four famous criteria including both pressure dependent and independent. The obtained results are in good agreement with experimental results. The consistent/continuum elastic-plastic moduli for Euler backward method are also investigated.

Keywords: Rate-independent Euler backward/forward methods; Consistent elastic-plastic modulus; Internally pressurized thick walled cylinder

1 INTRODUCTION

PLASTICITY describes the deformation of a material undergoing non-reversible changes of shape in response to applied forces. The main important of coding an elastic-plastic problem in a finite element program is how to update the state of stresses from $\left[t_n, t_{n+1}\right]$, where t_n is the first time and t_{n+1} is the end time of any load step. In general, there are four integration algorithm methods in updating stress, i.e. 1-exact integration algorithm methods, 2-explicit integration algorithm methods such as Euler forward method, 3-explicit/implicit integration algorithm methods and 4-implicit integration algorithm methods such as Euler backward method. The first one is more accurate which solves a first order plasticity differential equation because of the difficulty of the complicated problems the other three are in much attention especially the fourth one. The main point in associated plasticity is the direction of the incremental plastic strain with respect to the yield surface. If one accepts that direction to be normal to the yield surface at the beginning of the load step then the explicit integration algorithm methods is used, and the intersection point of the trial stress with the yield surface must be obtained. On the other hand, if the direction of the incremental plastic strain is normal to the yield surface at the end of the interval of the load step, the implicit integration algorithm methods are employed. In these algorithms, obtaining the intersection of the trials stresses with initial yield surface is unnecessary and it needs some trial and error iterations to reach normality at the end of load step. During the iterations, obtaining the second differentiation of the yield surface is necessary. Moreover, using an elastic-plastic modulus in global finite element procedure which is consistent with the linearized implicit algorithm is inevitable to preserve the quadratic rate of asymptotic convergence. To overcome these

* Corresponding author. Tel.: +98 9153111869; Fax: +98 511 8763304.
E-mail address: kadkhoda@um.ac.ir (M. Kadkhodayan).

difficulties, obtaining the second differentiation of a general yield surface can help to accomplish the numerical procedures. In explicit/implicit integration algorithm method , the direction of the incremental plastic strain from the values of the beginning and the end of the interval of the load step with the aid of different criteria can be evaluated.

Krieg and Krieg [1] investigated the accuracy of the integration of the constitutive equations for an isotropic elastic-perfectly plastic von Mises material. Schreyer et al. [2] examined tangent predictor-radial return approach and the elastic predictor–radial corrector algorithm with von Mises, isotropic hardening model under plane stress condition. Simo and Taylor [3] demonstrated that the concept of consistency between the tangent operator and the integration algorithm employed in the solution of the incremental problem plays a crucial role in preserving the quadratic rate of asymptotic convergence of iterative solution scheme based on Newton's method. Ortiz and Popov [4] investigated the accuracy and stability for integration of elastic-plastic constitutive relations. Potts and Gens [5] introduced five methods to treat this draft and recommended the 'correct' method in finite element calculations. Ortiz and Simo [6] proposed a new class of explicit integration algorithms for rate-independent and rate-dependent behaviors, with plastic hardening or softening, associated or non-associated flow rules and non-linear elastic response. Simo and Taylor [7] developed an unconditionally stable algorithm for plane stress elastoplasticity condition, based upon the concept of elastic predictor-return mapping (plastic corrector). Dodds [8] derived an extension of elastic-plastic-radial return algorithm and a consistent tangent operator which satisfy the requirements for stable, accurate and efficient numerical procedure for plane stress condition with mixed hardening. Ortiz and Martin [9] characterized the conditions under which an elastic-plastic stress update algorithm preserves the symmetries inherent to material response. Gratacos et al. [10] investigated the generalized midpoint rule for the time integration of elastic-plastic constitutive equations for pressure-independent yield criteria and the existence and uniqueness of the incremental solution was discussed. Ristinmaa and Tryding [11] introduced a unified approach to establish an exact integration of the constitutive equation in elastoplasticity, assuming the total strain-rate direction to be constant. Kadkhodayan and Zhang [12] proposed a new efficient method, the consistent DXDR method, to analyze general elastic-plastic problem.

In recent years, Foster et al. [13] modified spectral decomposition technique in implicit algorithms for models that include kinematic hardening for geomaterials. Kim and Gao [14] presented a general method to formulate the consistent tangent stiffness for plasticity. Hu and Wang [15] proposed a yield criterion with three independent invariants of the stress tensor and the deviatoric stress tensor to fulfill the experimental observations. Ding et al. [16] developed a stress integration scheme to analyze a three-dimensional sheet metal forming problems and implemented into ABAQUS/Explicit via User Material Subroutine (VUMAT) interface problem. Nicot and Darve [17] showed that employing regular flow rule for granular materials disappeared as soon as more general loading condition was applied. Their model highlighted the great influence of the loading history on the shape of the plastic Gudehus response-envelope. Oliver et al. [18] proposed an implicit/explicit scheme for non-linear constitutive scheme which provided an additional computability to those solid mechanics problems where robustness is an important issue. Ragione et al. [19] described the inelastic behavior of a granular material in the range of deformation that precedes localization by idealizing the material as a random array of identical, elastic, frictional spheres and assuming that particles moved with the average strain. Kossa and Szabo [20] presented semi-analytical solutions for the von Mises elastoplasticity by combined linear isotropic-kinematic hardening. Tu et al. [21] presented a semi-implicit return mapping algorithms for integrating generic non-smooth elastic-plastic models. Valoroso and Rosati [22] presented a general projected algorithm for general isotropic three-invariant plasticity method under plane stress conditions. Gao et al. [23] using experimental and numerical studies demonstrated that stress state had strong effects on both plastic response and ductile fracture behavior of an aluminum 5083 alloy. Cardoso and Yoon [24] derived a stress integration procedure based on the Euler backward method for a non-linear combined isotropic/kinematic hardening model based on the two-yield surfaces approach. Ghaei and Green [25] developed an algorithm for numerical implementation of Yoshida-Uemori two-surface plasticity model into finite element program with the aid of the return mapping procedure. Ghaei et al. [26] introduced a semi-implicit scheme to implement Yoshida-Uemori two-surface model into finite element method. Kossa and Szabo [27] proposed a new integration scheme for the von Mises elastic-plastic model with combined linear isotropic-kinematic hardening. Rezaiee-Pajand et al. [28] proposed two new exponential-based approximate formulations for associative Drucker-Prager criterion plasticity and could obtain the accurate solution of the problem. Becker [29] proposed a new plasticity algorithm based upon observation from the closed form integration of a generalized quadratic yield function over a single step.

Moayyedian and Kadkhodayan [30] presented a new first and second differentiation of a general yield surface and implemented it for different time stepping schemes including the explicit, trapezoidal implicit and fully implicit time stepping schemes in rate-dependant plasticity. Moayyedian and Kadkhodayan [31] presented a new non-associated viscoplastic flow rule (NAVFR) with combining von Mises and Tresca loci in place of yield and plastic potential functions and vice verse with the aid of fully implicit time stepping scheme.

Two important factors in integration algorithms are accuracy and stability. In explicit algorithms the size of load step plays a crucial role in stability and accuracy, i.e. a very large load step cannot guarantee the stability and accuracy of the algorithm. On the other hand, in the full implicit algorithms, even by choosing a large load step, the stability is guaranteed. In fact, this is the main advantage of implicit algorithms to explicit algorithms. However, choosing a large load step may not give a proper accuracy.

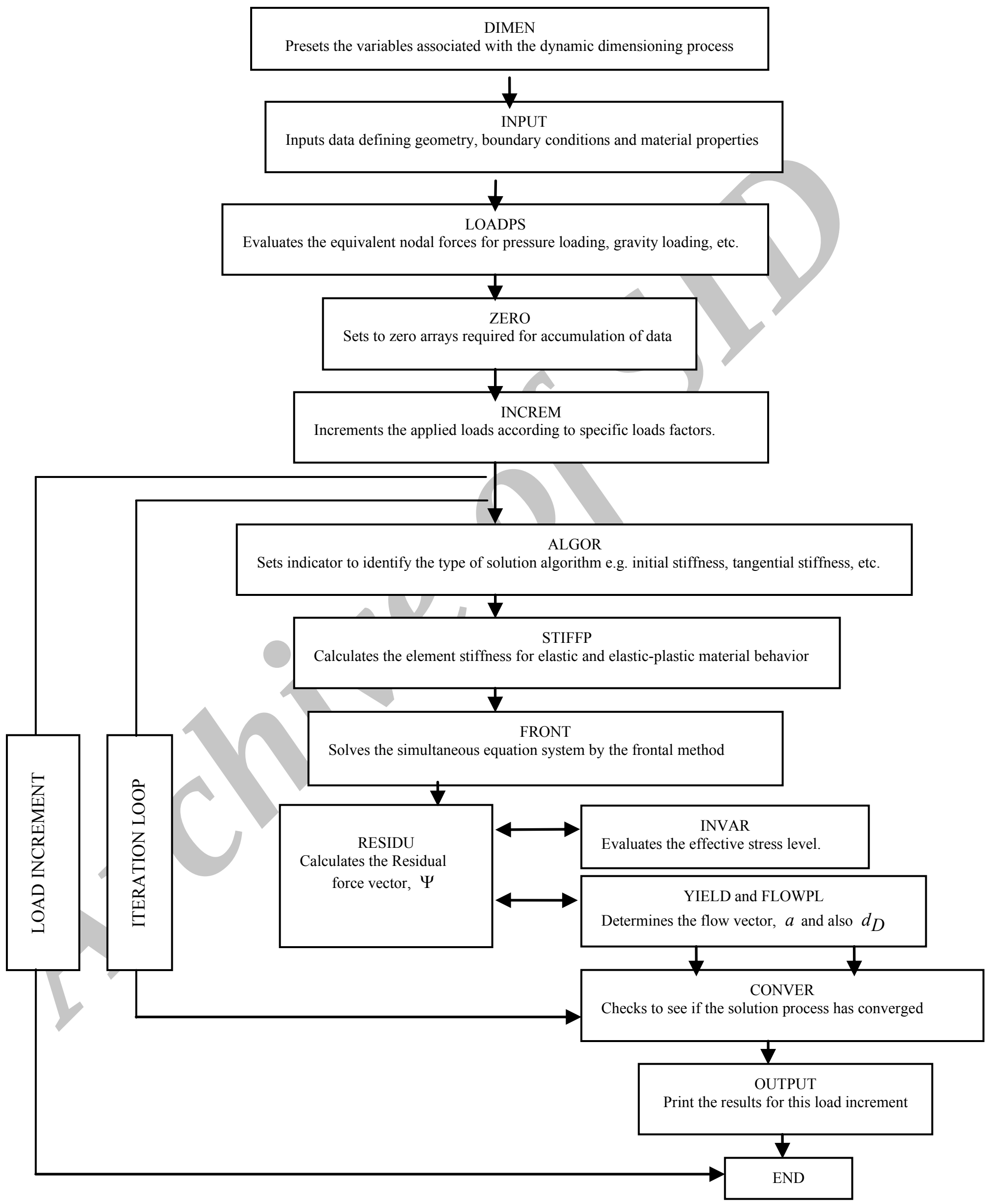

Fig. 1
Program flow chart for two-dimensional elastic-plastic applications [32].

In this paper, with the aid of obtained expressions for the first and second differentiation of a general yield surface in the previous work of the authors in [30] an internally pressurized thick walled cylinder is considered with perfectly plastic and linear-isotropic hardening behavior of material and coded in Compaq Visual Fortran

Professional Edition 6.5.0 with the aid of references [32-36] in finite element and [37-40] in plasticity theories. Euler forward method with sub-increment and Euler backward method along with the continuum and consistent elastic-plastic moduli with different criteria are investigated and the obtained results are compared to each other and experimental results. Fig. 1 shows the flow chart of the program for two-dimensional elastic-plastic applications for a global finite element.

2 EULER FORWARD (EXPLICIT) - MATRIX FORMULATION

The yield F can be written as:

$$F(\sigma,\kappa)=0, \tag{1}$$

where σ is the stress vector and κ is the hardening $d\kappa=\sigma^T d\varepsilon_p$ for the work hardening. Defining

$$\{a\}^T=\left[\frac{\partial F}{\partial\sigma_x},\frac{\partial F}{\partial\sigma_y},\frac{\partial F}{\partial\sigma_z},\frac{\partial F}{\partial\tau_{yz}},\frac{\partial F}{\partial\tau_{xz}},\frac{\partial F}{\partial\tau_{xy}}\right], \tag{2}$$

We have

$$\{d\sigma\}=\left[D_{ep}\right]\{d\varepsilon\}, \tag{3}$$

where

$$\left[D_{ep}\right]=\left[D\right]-\frac{\{d_D\}\{d_D\}^T}{H^{'}+\{d_D\}^T\{b\}},\quad \{d_D\}=\left[D\right]\{a\}. \tag{4}$$

Thus H' is obtained to be the local slope of the uniaxial stress/plastic strain curve and can be determined experimentally [30].

3 EULER BACKWARD (IMPLICIT), (GENERAL CLOSEST PONT PROJECTION) - MATRIX FORMULATION

For a linear-isotropic hardening in any load step we have

$$\sigma_{n+1}=\sigma_Y+H^{'}\left(\bar{\varepsilon}_{pn}+\Delta\lambda_{n+1}\right). \tag{5}$$

The yield function can take the following form

$$\begin{aligned}F_{n+1}&=F\left(\sigma_{n+1},\Delta\lambda_{n+1}\right)=f\left(\sigma_{n+1}\right)-k\left(\Delta\lambda_{n+1}\right)\\&=f\left(\sigma_{n+1}\right)-\left[\sigma_Y+H^{'}\left(\bar{\varepsilon}_{pn}+\Delta\lambda_{n+1}\right)\right]=0.\end{aligned} \tag{6}$$

The following steps have to be followed in a fully implicit algorithm.

1. Assume plastic loading, that is $F_{n+1}^{trial} > 0$, the plastic flow residual R_{n+1} and yield condition can be defined as:

$$\begin{cases} \left\{R_{n+1}\right\} = -\left\{\varepsilon_{n+1}^{p}\right\} + \left\{\varepsilon_{n}^{p}\right\} + \Delta\lambda_{n+1}\left\{a_{n+1}\right\}, \\ F_{n+1} = F\left(\sigma_{n+1}, \Delta\lambda_{n+1}\right), \end{cases} \tag{7}$$

where, $\left\{\sigma_{n+1}\right\} = \left[D\right]\left(\left\{\varepsilon_{n+1}\right\} - \left\{\varepsilon_{n+1}^{p}\right\}\right)$.

2. Linearized the above equation. Because ε_{n+1} and $d\bar{\varepsilon}_{pn}$ are assumed to be fixed during return-mapping stage, then $\left\{\Delta\varepsilon_{n+1}^{p}\right\}^{(k)} = -\left[D\right]^{-1}\left\{\Delta\sigma_{n+1}\right\}^{(k)}$ and we have:

$$\begin{cases} \left\{R_{n+1}\right\}^{(k)} + \left[\Xi_{n+1}\right]^{-1(k)}\left\{\Delta\sigma_{n+1}\right\}^{(k)} \\ +\left\{a_{n+1}\right\}^{(k)}\Delta^{2}\lambda_{n+1}^{(k)} = 0 \\ F_{n+1}^{(k)} + \left\{a_{n+1}\right\}^{T(k)}\left\{\Delta\sigma_{n+1}\right\}^{(k)} + H^{'}\Delta^{2}\lambda_{n+1}^{(k)} = 0, \end{cases} \tag{8}$$

and the Hessian matrix is:

$$\left[\Xi_{n+1}\right] = \left(\left[D\right]^{-1} + \Delta\lambda_{n+1}\left[\frac{\partial a_{n+1}}{\partial\sigma}\right]\right)^{-1}. \tag{9}$$

3. Solve the linearized problem to obtain $\Delta^{2}\lambda_{n+1}^{(k)}$ and $d\Delta\varepsilon_{n+1}^{p^{(k)}}$ as:

$$\begin{cases} \Delta^{2}\lambda_{n+1}^{(k)} = \dfrac{F_{n+1}^{(k)} - \left\{a_{n+1}\right\}^{T(k)}\left[\Xi_{n+1}\right]^{(k)}\left\{R_{n+1}\right\}^{(k)}}{\left\{a_{n+1}\right\}^{T(k)}\left[\Xi_{n+1}\right]^{(k)}\left\{a_{n+1}\right\}^{(k)} - H^{'}}, \\ \left\{\Delta\sigma_{n+1}^{(k)}\right\} = -\left[\Xi_{n+1}\right]^{(k)}\left[\left\{R_{n+1}\right\}^{(k)} + \right], \\ \left\{a_{n+1}\right\}^{(k)}\Delta^{2}\lambda_{n+1}^{(k)} \\ \left\{\Delta\varepsilon_{n+1}^{p^{(k)}}\right\} = -\left[D\right]^{-1} : \left\{\Delta\sigma_{n+1}^{(k)}\right\}. \end{cases} \tag{10}$$

4. Update the plastic strain $\left\{\varepsilon_{n+1}^{p^{(k)}}\right\}$ and the consistency parameter $\Delta\lambda_{n+1}^{(k)}$ as:

$$\left\{\varepsilon_{n+1}^{p}\right\}^{(k+1)} = \left\{\varepsilon_{n+1}^{p}\right\}^{(k+1)} + \left\{\Delta\varepsilon_{n+1}^{p}\right\}^{(k)}, \tag{11}$$

and

$$\Delta\lambda_{n+1}^{(k+1)} = \Delta\lambda_{n+1}^{(k)} + \Delta^{2}\lambda_{n+1}^{(k)}. \tag{12}$$

The procedure summarized above is simply a systematic application of Newton's method to the system of Eq. (10) that results in the computation of the closest point projection from trial state onto the yield surface. Note that in the Euler backward method normality is enforced at the final (unknown) iteration. The above procedure converged when $\sqrt{\{R_{n+1}\}^T\{R_{n+1}\}}$ and F_{n+1} in Eq. (7) reach to prescribed tolerances.

4 CONSISTENT ELASTIC-PLASTIC MODULUS - MATRIX FORMULATION

By differentiating the elastic stress-strain relationships and the discrete flow rule, we obtain

$$\begin{cases}\{d\sigma_{n+1}\}=[D]\left(\{d\varepsilon_{n+1}\}-\{d\varepsilon^p_{n+1}\}\right),\\ \{d\varepsilon^p_{n+1}\}=\Delta\lambda_{n+1}\left[\dfrac{\partial a_{n+1}}{\partial\sigma}\right]\{d\sigma_{n+1}\}+\\ d\Delta\lambda_{n+1}\{a_{n+1}\}.\end{cases} \tag{13}$$

The following algorithmic relationship is obtained:

$$\{d\sigma_{n+1}\}=[\Xi_{n+1}]\left(\{d\varepsilon_{n+1}\}-d\Delta\lambda_{n+1}\{a_{n+1}\}\right). \tag{14}$$

On the other hand, differentiating the discrete consistency condition yields

$$\{a_{n+1}\}^T\{d\sigma_{n+1}\}-H^{'}d\Delta\lambda_{n+1}=0. \tag{15}$$

Thus, from Eqs. (14) and (15) we have

$$\begin{aligned}&d\Delta\lambda_{n+1}=\frac{\{e_D\}^T\{d\varepsilon_{n+1}\}}{H^{'}+\{e_D\}^T\{a_{n+1}\}},\\ &\{e_D\}^T=\{a_{n+1}\}^T[\Xi_{n+1}].\end{aligned} \tag{16}$$

Finally, substituting Eq. (16) into Eq. (14) yields the expression for elastic-plastic relation

$$\{d\sigma_{n+1}\}=[D_{ep}]_{n+1}\{d\varepsilon_{n+1}\}, \tag{17}$$

where the consistent elastic-plastic modulus is defined as below

$$\begin{aligned}&[D_{ep}]_{n+1}=[\Xi_{n+1}]-\frac{\{e_D\}\{e_D\}^T}{H^{'}+\{e_D\}^T\{a_{n+1}\}},\\ &\{e_D\}=[\Xi_{n+1}]\{a_{n+1}\}.\end{aligned} \tag{18}$$

Note that the structure of Eq. (18) is analogous to Eq. (4). The elastic modulus $[D]$ as the continuum modulus in Eq. (4) is substituted by the algorithmic modulus $[\Xi_{n+1}]$ defined by Eq. (9). It should be noted that to compute $[\Xi_{n+1}]$ in Euler backward method to update stress state and construct the consistent elastic-plastic modulus, the derivation of the second differentiation of the yield surface is inevitable and for a complicated criteria is cumbersome where a comprehensive approach to overcome this difficulty was presented in the earlier work of the authors is employed in current research [30].

5 RESULTS AND DISCUSSIONS

In the following, different investigations and comparisons are achieved contained with the new expressions for differentiation of a general yield surface as in [30] for rate-independent plasticity:

1. Comparing between Euler forward and backward methods for four different criteria containing independent and dependant criteria to hydrostatic pressure.
2. Comparing the results obtained from Euler forward and backward methods with those of experimental data.
3. Comparing the continuum and consistent elastic-plastic moduli for Euler backward method.

Figs. 1 and 2 show the variation of circumferential strain and stress at the inner surface with the internal pressure while the von Mises criterion, perfect-plastic material and also linear isotropic hardening behavior such that $H' = \frac{E}{10}$ are used. The geometry of the cylinder is assumed as *b*/*a*=2. The variations of circumferential strain of the inner surface (*r*/*a*=1) with pressure and also circumferential stress distributions in the interval of $(1 \le r/a \le 2)$ for Euler forward and backward methods are considered here. Fig. 2 shows that with increasing the pressure and development of plastic zone, the differences between the results of Euler forward and backward methods increase. Moreover, in the same pressure, the hoop strain predicted by the implicit integration algorithm is larger than that of explicit one. In addition, the hoop stress predicted by Euler backward method is smaller than that of Euler forward method, Fig. 3. Furthermore, the results show that the material hardening increases the difference between two integration algorithm methods. Figs. 4, 5, 6, 7 and 8, 9 show the same parameters based on Tresca, Mohr-Coulomb and Drucker-Prager criteria, respectively. In using Mohr-Coulomb criterion it is assumed that $tan\Phi = 0.879$ and for the linear isotropic hardening material $H' = E/20$ and in Drucker-Prager criteria it is assumed that $H' = E/(10\sqrt{3})$.

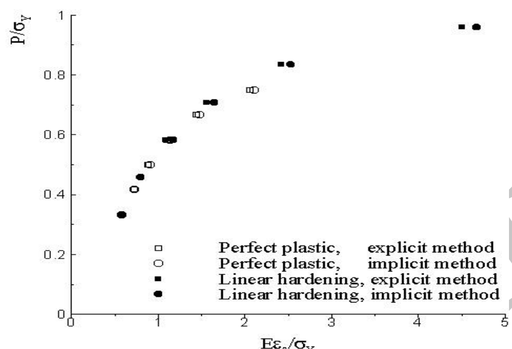

Fig. 2
Circumferential strain of the inner surface with increasing pressure using von Mises criterion.

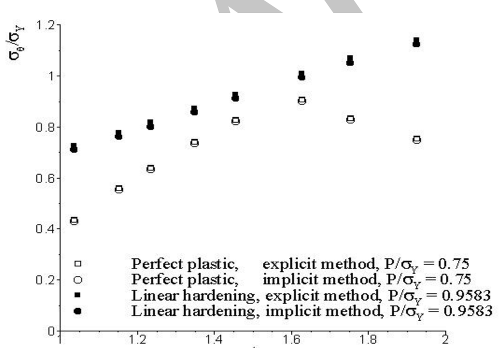

Fig. 3
Circumferential stress distributions using von Mises criterion.

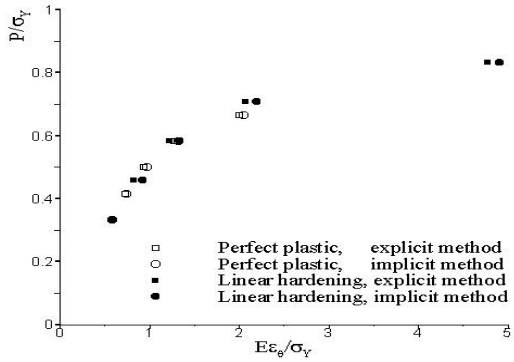

Fig. 4
Circumferential strain of the inner surface with increasing pressure using Tresca criterion.

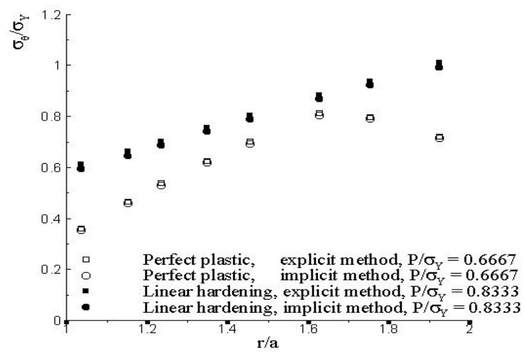

Fig. 5
Circumferential stress distributions using Tresca criterion.

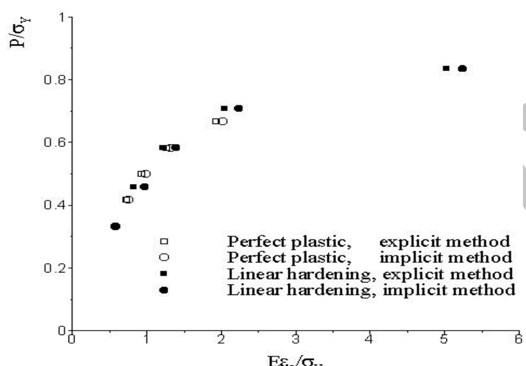

Fig. 6
Circumferential strain of the inner surface with increasing pressure using Mohr-Coulomb criterion.

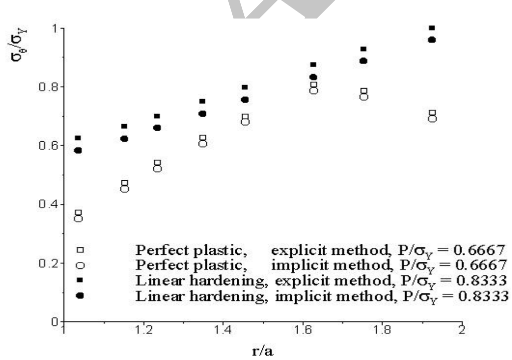

Fig. 7
Circumferential stress distributions using Mohr-Coulomb criterion.

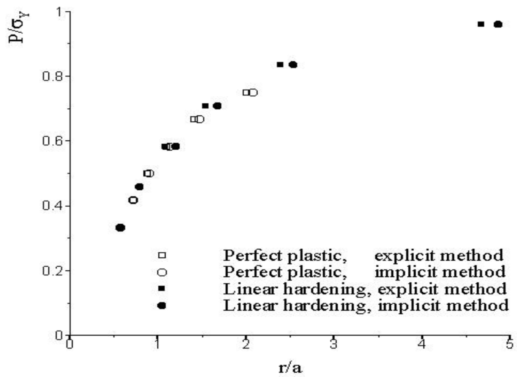

Fig. 8
Circumferential strain of the inner surface with increasing pressure using Drucker-Prager criterion.

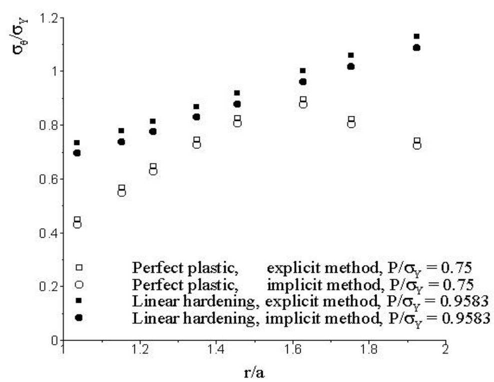

Fig. 9
Circumferential stress distributions using Drucker-Prager criterion.

The results show the same trend as explained for Figs. 2 and 3 previously. The results show the differences between the explicit and implicit integration algorithm methods in Mohr-Coulomb and Drucker-Prager criteria are larger than those in Tresca and von Mises criteria, respectively. In other words, when the yielding criteria are dependent to the hydrostatic pressure, the differences between the results obtained from the Euler forward and backward methods are more significant than those of the hydrostatic pressure independent yielding criteria. Furthermore, it can be shown that in non-linear isotropic hardening materials these differences increase compared with perfect-plastic materials. Table 1. shows the required iteration number for converged results when the consistent and continuum elastic-plastic moduli in Euler backward method are used. As it is seen, the required iterations in each increment for consistent elastic-plastic modulus is less than that of the continuum one, i.e. the former preserves the asymptotic rate of quadratic convergence in implicit integration algorithm. Moreover, the Mohr-Coulomb and von Mises criteria have the highest and the lowest required number of iterations, respectively.

Furthermore, the number of required iterations increases when plastic zone is developed. In perfect-plastic materials, in addition, the number of iterations in last increments increases which can be attributed to the initiation of some kinds of instability in this type of material. It is also observed that employing the consistent elastic-plastic modulus instead of the continuum one causes more decreasing in required iteration number in hydrostatic pressure dependent yielding criteria compared to independent ones. Finally, employing the consistent elastic-plastic modulus with Euler backward method for non-circular shape criteria in deviatoric plane needs more iteration in each load step.

Fig.10 show a comparison between the results obtained by Euler forward and backward methods and experimental results. The figure demonstrates the variations of internal pressure in over strain 100% $(E\varepsilon_\theta / \sigma_Y = 1)$ at external surface of the vessel with the ratio of external radius/internal radius, (b/a), for perfect-plastic material and von Mises criterion. It is seen that using Euler backward method could predict the experimental result more accurately. It is also observed that differences between the numerical simulations and experimental data are maximum in b/a=1.6 and minimum in b/a=2.4. It should be noted the results agree with the results in [30] too.

Table 1
The number of required iteration in each load step using, (a) von Mises criterion, (b) Tresca criterion, (c) Mohr-Coulomb criterion, (d) Drucker-Prager criterion.

(a)

	von Mises criterion and perfect-plastic material					
Step	1	2	3	4	5	6
State	el	el-el	el-pl	pl-pl	pl-pl	pl-pl
Continuum	1	1	2	3	5	8
Consistent	1	1	2	2	3	5

	von Mises criterion and linear isotropic hardening material					
Step	1	2	3	4	5	6
State	el	el-el	el-pl	pl-pl	pl-pl	pl-pl
Continuum	1	1	3	4	5	7
Consistent	1	1	2	2	3	4

(b)

	Tresca criterion and perfect-plastic material				
Step	1	2	3	4	5
State	el	el-pl	pl-pl	pl-pl	pl-pl
Continuum	1	3	3	6	9
Consistent	1	2	2	3	5

	Tresca criterion and linear isotropic hardening material				
Step	1	2	3	4	5
State	el	el-pl	pl-pl	pl-pl	pl-pl
Continuum	1	4	4	5	9
Consistent	1	2	3	3	4

(c)

	Mohr-Coulomb criterion and perfect-plastic material				
Step	1	2	3	4	5
State	el	el-pl	pl-pl	pl-pl	pl-pl
Continuum	1	4	6	8	11
Consistent	1	2	3	4	6

	Mohr-Coulomb criterion and linear isotropic hardening material				
Step	1	2	3	4	5
State	el	el-pl	pl-pl	pl-pl	pl-pl
Continuum	1	4	7	8	10
Consistent	1	2	3	3	5

(d)

	Drucker-Prager criterion and perfect-plastic material					
Step	1	2	3	4	5	6
State	el	el-el	el-pl	pl-pl	pl-pl	pl-pl
Continuum	1	1	4	5	7	10
Consistent	1	1	2	2	4	5

	Drucker-Prager criterion and linear isotropic hardening material					
Step	1	2	3	4	5	6
State	el	el-el	el-pl	pl-pl	pl-pl	pl-pl
Continuum	1	1	4	6	6	9
Consistent	1	1	3	3	3	4

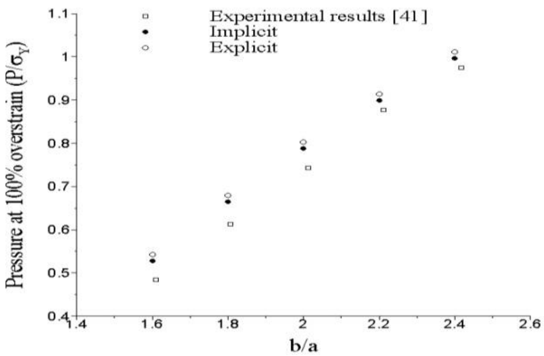

Fig. 10
Comparison between the Euler forward/backward methods and experimental data.

6 CONCLUSIONS

A new procedure with using newly obtained first and second differentiation of a yield function [30] is implemented for Euler forward and backward method in rate-independent plasticity. In the following, some more obtained results are explained:

1. Applying more loads and development of plastic zone make the differences between the obtained results from Euler forward and backward and also continuum and consistent operators more obvious.
2. It was demonstrated that the hydrostatic pressure dependent yield criteria continuum and consistent elastic-plastic moduli were more sensitive in employing Euler forward and backward methods.
3. Comparing the results obtained from von Mises and Tresca and also Drucker-Prager and Mohr-Coulomb criteria show that employing consistent elastic-plastic modulus in implicit integration algorithm for non-circular surfaces in deviatoric plane needs more number of iterations to converge.

REFERENCES

[1] Krieg R.D., Krieg D.B., 1977, Accuracies of numerical solution methods for the elastic-perfectly plastic model, *Journal of Pressure Vessel Technology -Transactions of the ASME* **99**:510-515.

[2] Schreyer H.L., Kulak R.F., Kramer J.M., 1979, Accurate numerical solutions for elastic-plastic models, *Transactions of the ASME* **101**: 226-234.

[3] Simo J.C., Taylor R.L., 1985, Consistent tangent operators for rate-independent elastoplasticity, *Computer Methods in Applied Mechanics and Engineering* **48**:101-118.

[4] Ortiz M., Popov E.P., 1985, Accuracy and stability of integration algorithms for elastoplastic constitutive relations, *International Journal for Numerical Methods in Engineering* **21**:1561-1576.

[5] Potts D.M., Gens A., 1985, A critical assessment of methods of correcting for draft from the yield surface in elasto-plastic finite element analysis, *International Journal for Numerical and Analytical Methods in Geomechanics* **9**:149-159.

[6] Ortiz M., Simo J.C., 1986, An analysis of a new class of integration algorithms for elastoplastic constitutive relations, *International Journal for Numerical Methods in Engineering* **23**:353-366.

[7] Simo J.C., Taylor R.L., 1986, A return mapping algorithm for plane stress elastoplasticity, *International Journal for Numerical Methods in Engineering* **38**:649-670.

[8] Dodds R.H., 1987, Numerical techniques for plasticity computations in finite element analysis, *Computers & Structures* **26**:767-779.

[9] Ortiz M., Martin J.B., 1989, Symmetry-preserving return mapping algorithms and incrementally external paths: A unification of concepts, *International Journal for Numerical Methods in Engineering* **28**:1839-1853.

[10] Gratacos P., Montmitonnet P., Chenot J.L., 1992, An integration scheme for Prandtl-Reuss elastoplastic constitutive equations, *International Journal for Numerical Methods in Engineering* **33**:943-961.

[11] Ristinmma M., Tryding J., 1993, Exact integration of constitutive equations in elasto-plasticity, *International Journal for Numerical Methods in Engineering* **36**:2525-2544.

[12] Kadkhodayan M., Zhang L.C., 1995, A consistent DXDR method for elastic-plastic problems, *International Journal for Numerical Methods in Engineering* **38**:2413-2431.

[13] Foster C.D., Regueiro R.A., Fossum A.F., Borja R.I., 2005, Implicit numerical integration of a three-invariant, isotropic/kinematic hardening cap plasticity model for geomaterials, *Computer Methods in Applied Mechanics and Engineering* **194**:5109-5138.

[14] Kim J., Gao X., 2005, A generalised approach to formulate the consistent tangent stiffness in plasticity with application to the GLD porous material model, *International Journal of Solid and Structures* **42**:103-122.

[15] Hu W., Wang Z.R., 2005, Multiple-factor dependence of the yielding behaviour to isotropic ductile material, *Computational Materials Science* **32**:31-46.

[16] Ding K.Z., Qin Q.H., Cardew-Hall M., 2007, Substepping algorithms with stress correction for simulating of sheet metal forming process, *International Journal of Mechanical Sciences* **49**:1289-1308.

[17] Nicot F., Darve F., 2007, Basic features of plastic strains: from micro-mechanics to incrementally nonlinear models, *International Journal of Plasticity* **23**:1555-1588.

[18] Oliver J., Huespe A.E., Cante J.C., 2008, An implicit/explicit integration scheme to increase computability of non-linear material and contact/friction problems, *Computer Methods in Applied Mechanics and Engineering* **197**:1865-1889.

[19] Ragione L.L., Prantil V.C., Sharma I., 2008, A simplified model for inelastic behaviour of an idealized granular material, *International Journal of Plasticity* **24**:168-189.

[20] Kosa A., Szabo L., 2009, Exact integration of the von mises elastoplasticity model with combined linear isotropic/kinematic hardening, *International Journal of Plasticity* **25**:1083-1106.

[21] Tu X., Andrade J.E., Chen Q., 2009, Return mapping for nonsmooth and multiscale elastoplasticity, *Computer Methods in Applied Mechanics and Engineering* **198**:2286-2296.

[22] Valoroso N., Rosti L., 2009, Consistent derivation of the constitutive algorithm for plane stress isotropic plasticity, *International Journal of Solid and Structures* **46**:74-91.

[23] Gao X., Zhang T., Hayden M., Roe C., 2009, Effects of the stress state on plasticity and ductile failure of an aluminium 5083 alloy, *International Journal of Plasticity* **25**:2366-2382.

[24] Cardoso R.P.R., Yoon J.W., 2009, Stress integration method for a nonlinear kinematic/isotropic hardening model and its characterization based on polycrystal plasticity, *International Journal of Plasticity* **25**: 1684-1710.

[25] Ghaie A., Green D.E., 2010, Numerical implementation of Yoshida-Uemori two-surface plasticity model using a fully implicit integration scheme, *Computational Material Sciences* **48**:195-205.

[26] Ghaei A., Green D.E., Taherizadeh A., 2010, Semi-implicit numerical integration of Yoshida-Uemori two-surface plasticity model, *International Journal of Mechanical Sciences* **52**:531-540.

[27] Kossa A., Szabo L., 2010, Numerical implementation of a novel accurate stress integration scheme for the von Mises elastoplasticity model with combined linear hardening, *Finite Element in Analysis and Design* **46**:391-400.

[28] Rezaiee-Pajand M., Sharifan M., 2011, Accurate and approximate integrations of Drucker-Prager plasticity with linear isotropic and kinematic hardening, *European Journal of Mechanics A/Solids* **30**:345-361.

[29] Becker R., 2011, An alternative approach to integrating plasticity relations, *International Journal of Plasticity* **27**:1224-1238.

[30] Moayyedian F., Kadkhodayan M., 2013, A general solution in Rate-Dependant plasticity, *International Journal of Engineering* **26**:391-400.

[31] Moayyedian F., Kadkhodayan M., 2014, A study on combination of von mises and tresca yield loci in non-associated viscoplasticity, *International Journal of Engineering* **27**:537-545.

[32] Owen D.R.J., Hinton E., 1980, *Finite Elements in Plasticity: Theory and Practice*, Pineridge Press Limited.

[33] Souza Neto E.D., Peric D., Owen D.R.J., 2008, *Computational Methods for Plasticity, Theory and Applications*, John Wiley and Sons, Ltd.

[34] Simo J.C., Hughes T.J.R., 1998, *Computational Inelasticity*, Springer-Verlag New York, Inc.

[35] Zienkiewicz O.C., Taylor R.L., 2005, *The Finite Element Method for Solid and Structural Mechanics*, Elsevior Butterworth-Heinemann, sixth edition.

[36] Crisfield M.A., 1997, *Non-Linear Finite Element Analysis of Solids and Structures*, New York , John Wiley.

[37] Hill R., 1950, *The Mathematical Theory of Plasticity*, Oxford University Press, New York.

[38] Chakrabarty J., 1987, *Theory of Plasticity*, McGraw-Hill, New York.

[39] Chen W.F., Zhang H., 1936, *Structural Plasticity Theory*, *Problems and CAE Software*, Springer-Verlag, New York.

[40] Khan A., Hung S., 1995, *Continuum Theory of Plasticity*, John Wiley & Sons, Canada.

[41] Marcal P.V., 1965, A note on the elastic-plastic thick cylinder with internal pressure in the open and closed-end condition, *International Journal of Mechanical Sciences* **7**:841-845.